Applied Catalysis B: Environmental 126 (2012) 186–199

Contents lists available at SciVerse ScienceDirect

Applied Catalysis B: Environmental

journal homepage: www.elsevier.com/locate/apcatb

Effect of H_2S on the behaviour of an impregnated NiO-based oxygen-carrier for chemical-looping combustion (CLC)

Cristina Dueso, María T. Izquierdo, Francisco García-Labiano*, Luis F. de Diego, Alberto Abad, Pilar Gayán, Juan Adánez

Instituto de Carboquímica (ICB-CSIC), Department of Energy and Environment, Miguel Luesma Castán 4, 50018 Zaragoza, Spain

ARTICLE INFO

Article history:
Received 22 February 2012
Received in revised form 3 July 2012
Accepted 16 July 2012
Available online 24 July 2012

Keywords:
Chemical-looping combustion (CLC)
Oxygen-carrier
Nickel oxide
Sulphur

ABSTRACT

Gaseous fuels for chemical-looping combustion (CLC) process may contain sulphur-compounds which could affect the oxygen-carrier behaviour, especially if NiO is used as active phase. In this work, several samples of a NiO-based oxygen-carrier prepared by impregnation (18 wt.%) on α-Al_2O_3, so-called NiO18-αAl, were extracted from a CLC unit after continuous operation with CH_4 containing 500 vppm of H_2S and characterized subsequently. Part of the sulphur fed to the system was release as SO_2 in the air-reactor during the CLC experiments while the rest remained in the solid particles. Ni_3S_2 was found in the oxygen-carrier extracted from the fuel-reactor, although small amounts of $NiSO_4$ were also detected. On the contrary, $NiSO_4$ was the main sulphur compound in the oxygen-carrier from the air-reactor while a low concentration of Ni_3S_2 was present. Despite the accumulated sulphur and the oxygen transport capacity loss during the operation, the oxygen-carrier was capable of recovering the initial reactivity for the CH_4 combustion after some time without H_2S feeding to the CLC system. In addition, a study about the possible regeneration of the oxygen-carrier in the air-reactor working at different temperatures and oxygen concentrations was performed. Independently of the operating conditions, part of the sulphur remained in the solid and total regeneration was not possible. The analysis of the NiO18-αAl oxygen-carrier after the CLC operation using TPR and XPS techniques revealed that sulphur reacted preferably with free NiO instead of $NiAl_2O_4$. Although Ni_3S_2 was the majority sulphide in the fuel-reactor, minor amounts of other sulphides such as NiS were detected. Sulphur was preferably concentrated in the outer surface of the particles. Taking into account all these results, a previous desulphuration process of the fuel would be necessary when NiO-based oxygen-carriers are used in a CLC system.

1. Introduction

During last decades, negative effects of global warming have been a constant source of concern to the scientific community. Huge research efforts have been done trying to turn the trend of the increasing greenhouse gas emissions to the atmosphere, primarily CO_2. Since about a third of the global CO_2 emissions come from the burning of fossil fuels for power generation [1] and a significant change in the dependence on this kind of fuels is not expected in the near future, CO_2 capture and storage in geological formations has emerged as a possible solution to reduce anthropogenic emissions. A large number of processes which accomplish the capture of CO_2 from combustion sources are currently available or under development, i.e. pre-combustion, post-combustion or oxyfuel technologies. Nevertheless, most of these techniques have several drawbacks as the high cost and energy consumption and, therefore, a decrease in the global efficiency of the energy generation process.

Within this framework, chemical-looping combustion (CLC) has been identified as a promising technology for clean combustion of fossil fuels. CO_2 capture is inherent to the process and, hence, any separation step or additional energy is not needed to produce a pure CO_2 stream ready for sequestration. A metal oxide acts as an oxygen-carrier circulating between two fluidized-bed reactors, the fuel- and the air-reactor, and transports the oxygen from the combustion air to the fuel, thus avoiding the dilution of flue gases with the N_2 of the air. In the fuel-reactor, the fuel gas (C_nH_{2m}) is oxidized to CO_2 and H_2O by the metal oxide which is reduced to a metal or the reduced form of the oxide at the same time. Almost pure CO_2 can be obtained after H_2O condensation. The metal or reduced oxide is regenerated with air in the air-reactor. Only N_2 and unreacted O_2 are released from this reactor. Although the reduction reaction can be exothermic or endothermic depending on the type of metallic oxide and the fuel, and the oxidation reaction is always

* Corresponding author. Tel.: +34 976 733 977; fax: +34 976 733 318.
E-mail address: glabiano@icb.csic.es (F. García-Labiano).

0926-3373/$ – see front matter © 2012 Elsevier B.V. All rights reserved.
http://dx.doi.org/10.1016/j.apcatb.2012.07.011

exothermic, the total amount of heat generated in the CLC system is the same as in conventional combustion where the air and the fuel are mixed.

Several transition state metals, such as Ni, Cu, Mn, Fe and Co, have been proposed as the most suitable materials for CLC [2–4]. The metal oxide is usually supported on an inert material, which increases its mechanical strength and provides a higher surface area for the reaction. Oxygen-carriers prepared over Al_2O_3, SiO_2, TiO_2 and yttrium stabilized zirconia (YSZ) as binders can be found in the literature. NiO-based oxygen-carriers have attracted most research interest for gas combustion due to their high reactivity with methane, main component of natural gas and refinery gas [5–8], and their thermal stability. More than 20 different oxygen-carriers based on nickel oxide have been investigated in different CLC continuous units from 300 W_{th} to 140 kW_{th} for 2500 h [2], showing very high combustion efficiencies. Nevertheless, thermodynamic restrictions avoid full conversion of the fuel into CO_2 and H_2O and small CO and H_2 concentrations can be found in the outlet gas stream from the fuel-reactor of the CLC system. The use of Al_2O_3 as support for NiO-based oxygen-carriers has been widely studied in the literature due to its good fluidization properties and thermal stability. However, a drawback of this material is $NiAl_2O_4$ formation [9]. At high calcination temperatures (>1073 K), part of NiO can react with the alumina to form nickel aluminate [10], which has lower reactivity than free NiO.

Gaseous fuels for the CLC process, such as natural gas, refinery gas or synthesis gas from coal gasification, may contain different amounts of impurities, like sulphur in the form of H_2S or COS, which could interact with the metallic oxide, thus affecting the performance of the CLC system. Although the H_2S concentration in the natural gas is usually quite low (≈20 vppm) [11], the content of this compound may reach values of 800 vppm in a refinery gas [12] and even 8000 vppm in a raw synthesis gas [13]. Sulphur in the fuel could react with the metallic oxide in the oxygen-carrier to form sulphur-containing compounds, such as sulphides and sulphates, that could decrease the oxygen-carrier reactivity and, as a consequence, the energy efficiency of the process. Moreover, the low melting point of some sulphides could produce the agglomeration of the particles and affect the solids circulation pattern between the interconnected fluidized bed reactors [10].

Although the poisoning effect of sulphur for Ni catalysts is especially well-known and many works about this issue can be found in the literature, not many articles about the effect of sulphur on oxygen-carriers for the CLC process have been published up to now. First, several thermodynamic studies appeared. Mattisson et al. [10] determined that H_2S could be partially oxidized to SO_2 in the fuel-reactor using a NiO-based oxygen-carrier and CH_4 as fuel, improving the conversion degree at high temperatures and low pressures. Both gaseous compounds, SO_2 and H_2S, could react with nickel in the particles to form Ni_3S_2, the most stable sulphide. Nickel sulphate was not present under the reducing fuel-reactor conditions. Later, Jerndal et al. [14] investigated the thermodynamics of oxygen-carriers based on Ni, Cu, Fe, Mn, Co, W and sulphates of Ba and Sr regarding carbon deposition and formation of sulphides and sulphates using CH_4, H_2 and CO as fuels. The same results were found with respect to the nickel behaviour in the presence of sulphur. Wang et al. [15] also studied carbon deposition and sulphur effect on the performance of oxygen-carriers based on five metal oxides (NiO, CuO, Fe_2O_3, Mn_3O_4 and CoO) through thermodynamic simulations using syngas as fuel and they again observed the tendency of nickel to react with the sulphur to form Ni_3S_2 in the particles.

More recently other authors presented studies performed in thermobalance (TGA) and CLC pilot plants [16–20]. They found that, although the presence of H_2S affected the reaction rates and reactivities of the oxygen-carriers, the formation of sulphides was completely reversible and SO_2 was released in the outlet stream from the air-reactor. Forero et al. [21] analysed the behaviour of a Cu-based oxygen-carrier prepared by impregnation in a 500 W_{th} CLC continuous unit. Most of the sulphur fed to the system was oxidized to SO_2 in the fuel-reactor and emitted in the outlet stream of this reactor (≈95%). Nevertheless, a small amount of sulphur reacted with the solid to form Cu_2S, which was transferred to the air-reactor with the particles and oxidized there to SO_2 with the oxygen of the air. No deactivation of the oxygen-carrier was observed even working with high H_2S concentrations (1300 vppm). Mayer [22] investigated the performance of a mixture of two nickel-based oxygen-carriers (N-VITO and N-VITO Mg) prepared by spray drying in a 120 kW_{th} CLC unit using natural gas containing 48 vppm of H_2S. A decrease in the combustion efficiency was observed during the sulphur treatment, but the oxygen-carrier was regenerated when H_2S feeding stopped.

In previous works carried out at ICB-CSIC, an impregnated oxygen-carrier supported on α-Al_2O_3 with 18 wt% of NiO, so-called NiO18-αAl, had been successfully used in a CLC continuous plant with CH_4 [23] and syngas [24] as fuels. This material showed suitable properties to be considered as oxygen-carrier for CLC process. The behaviour of this solid in the presence of impurities in the fuel, such as hydrocarbons [25] and sulphur [26], was also studied. Several tests with different H_2S concentrations (100–1000 vppm) in the fuel (CH_4) and temperatures (1103–1153 K) were carried out in a 500 W_{th} continuous plant. During these experiments, a loss of reactivity was always detected, although it had low relevance for H_2S concentrations below 100 vppm. In addition, a compilation of possible reactions involving sulphur in CLC was made according to the gaseous sulphur species obtained at the outlet stream from the air and the fuel-reactor and the assumed solid compounds formed on the oxygen-carrier. H_2S and SO_2 were found at very low concentrations (<10 vppm) in the fuel-reactor outlet stream but sulphur reacted with NiO to form Ni_3S_2. This compound was transferred to the air-reactor where it reacted with the air to produce SO_2 or $NiSO_4$ depending on the temperature. A mass balance to the system also indicated a gradual accumulation of sulphur in the oxygen-carrier particles.

One goal of the current work is to find out which sulphur components are present in the NiO18-αAl oxygen-carrier after CH_4 combustion tests in the presence of H_2S in a 500 W_{th} continuous CLC unit and hence to verify if the mechanism proposed in [26] is applicable. Moreover, the possible oxygen-carrier regeneration was also analysed, determining the effect of temperature and oxygen concentration in the air-reactor. The most suitable situation for the industrial CLC operation with Ni-based oxygen-carriers would be the total release of the sulphur introduced in the fuel as SO_2 in the air-reactor, in order to keep a high reactivity of the oxygen-carrier during the operation time. Different characterization techniques such as temperature programmed reduction and oxidation (TPR/TPO) and X-ray photoelectron spectroscopy (XPS) were used in order to determine the sulphur compounds present in the oxygen-carrier particles and their degree of interaction with the support.

2. Experimental

2.1. Oxygen-carrier

A nickel-based oxygen-carrier, so-called NiO18-αAl, was used in this work. The desired NiO content in the solid, 18 wt.%, was obtained by applying two successive steps of hot incipient wet impregnation on an α-Al_2O_3 support, as described by Gayán et al. [27]. The α-Al_2O_3 support particles (100–300 μm) were prepared by calcination of commercial γ-Al_2O_3 (Puralox NWa-155, Sasol

Table 1
Properties of the fresh NiO18-αAl oxygen-carrier.

NiO content (wt.%)	18
Particle size (μm)	100–300
Apparent density (g/cm^3)	2.5
BET surface area (m^2/g)	7
Porosity (%)	43
Mechanical strength (N)	4.1
XRD phases	α-Al_2O_3, NiO, $NiAl_2O_4$
Oxygen transport capacity	0.04

Germany GmbH) at 1423 K for 2 h. Table 1 shows the main properties of the fresh oxygen-carrier. The oxygen transport capacity was defined as the mass fraction of oxygen that can be used in the oxygen transfer, calculated as $R_{OC} = (m_{ox} - m_{red})/m_{ox}$, where m_{ox} and m_{red} are the masses of the oxidized and reduced forms of the oxygen-carrier, respectively.

In the experiments carried out in this work, two different types of sulphur-containing samples were used. The first one corresponds to samples obtained after operation in a continuous CLC plant using CH_4 in the presence of H_2S as fuel, while the second one was made up of sulphided particles prepared in a batch fluidized bed. More details about these samples can be found below.

2.2. CLC prototype (500 W_{th})

The schematic diagram of the 500 W_{th} chemical-looping combustion prototype used for the experimental tests is shown in Fig. 1. The total solid inventory in the system was about 1.3 kg of oxygen-carrier.

The fuel-reactor consisted in a bubbling fluidized bed (0.05 m i.d.) with a bed high of 0.1 m. In this reactor, the CH_4 reacts with

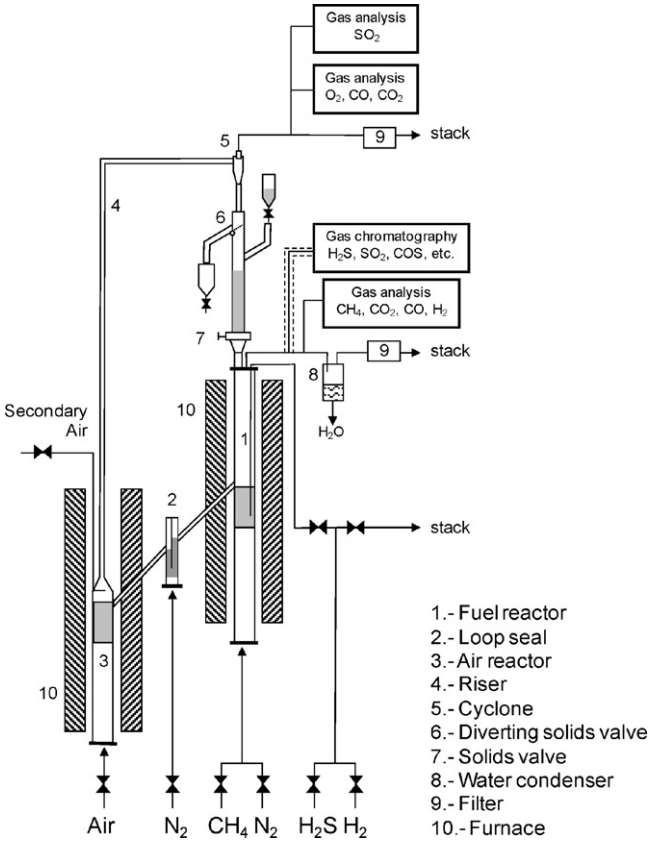

Fig. 1. Schematic diagram of the 500 W_{th} CLC prototype used for the tests with H_2S feeding.

the oxygen-carrier to give CO_2 and H_2O. The solids reduced in the fuel-reactor were then transported to the air-reactor through a nitrogen-flowing loop seal to prevent the mixing of the fuel gas in fuel-reactor and the oxygen in air-reactor while solids were flowing through it. The air-reactor was a bubbling fluidized bed (0.05 m i.d.) whose bed height was 0.1 m, followed by a riser of 0.02 m i.d. and 1 m height. The fully oxidized carrier was recovered by a high-efficiency cyclone, and sent to a solid reservoir, ready to start a new cycle. A solid valve situated below the cyclone allowed the measurements of the solid flow rates. Fine particles formed by attrition/fragmentation during operation were recovered in both the cyclones and the filters located in the fuel-reactor and air-reactor lines.

The prototype had several tools of measurement and system control. Thermocouples and pressure drop transducers located at different points of the plant showed the current operating conditions at any time. Specific mass flow controllers gave accurate flow rates of feeding gases. The gaseous outlet streams of the fuel-reactor and air-reactor were drawn to respective on-line gas analyzers to get continuous data of the gas composition. CH_4, CO, H_2 and CO_2 concentrations in the gas outlet stream from the fuel-reactor were measured after steam condensation. O_2, CO and CO_2 concentrations were obtained at the gas outlet stream from the air-reactor. CH_4, CO and CO_2 concentrations were measured by non-dispersive infrared (NDIR) analyzers (Maihak S710/UNOR), O_2 concentration was determined using a paramagnetic analyzer (Maihak S710/OXOR-P), and H_2 concentration by a thermal conductivity detector (Maihak S710/THERMOR). All data were collected by means of a data logger connected to a computer.

To study the effect of sulphur on the oxygen-carrier, the CLC pilot plant was modified including two mass flow controllers for H_2S and H_2. Small amounts of H_2 were used to avoid the decomposition of H_2S in the feeding lines. Some specific analyzers for sulphur compounds were used for the outlet streams of the fuel and air-reactors. A non-dispersive infrared (NDIR) analyzer (Siemens Ultramat U22) was used to detect the SO_2 concentrations obtained at the air-reactor gas outlet stream. For the analysis of the fuel-reactor gas, NDIR analyzers showed problems of cross-interference between gases. Thus, a gas chromatograph (Varian 3400-CX GC) equipped with a PORAPAK-Q packed column for chromatographic separation and a sulphur-specific flame photometric detector (FPD) was used. In this way, it was possible the detection of the different gaseous sulphur compounds that can appear in the fuel-reactor as H_2S, SO_2, COS, CS_2, etc. The chromatograph was calibrated in the range 0–200 vppm for H_2S and SO_2.

Moreover, the prototype allowed the collection of solid material samples from the air-reactor and the riser line at any moment from the diverting solid valve, and from the fuel-reactor at the end of the test.

2.3. Batch fluidized bed reactor

Fig. 2 shows the scheme of the batch fluidized bed installation, which has been previously used for determining agglomeration and attrition properties of several oxygen-carriers [28]. It consisted of a system for gas feeding, a fluidized bed reactor and a gas analysis system. The fluidized bed reactor was 0.054 m i.d. and 0.5 m height, with a 0.3 m of preheating zone just under the distributor. The reactor had two connected pressure taps in order to measure the differential pressure drop in the bed. A small hopper located in the upper part of the reactor allowed introducing solid samples to the system. A non-dispersive infrared analyser (NDIR) Siemens ULTRAMAT U22 allowed measuring the SO_2 concentration continuously.

This set up was used for several applications: (1) to determine and quantify the presence of nickel sulphides and sulphates in the

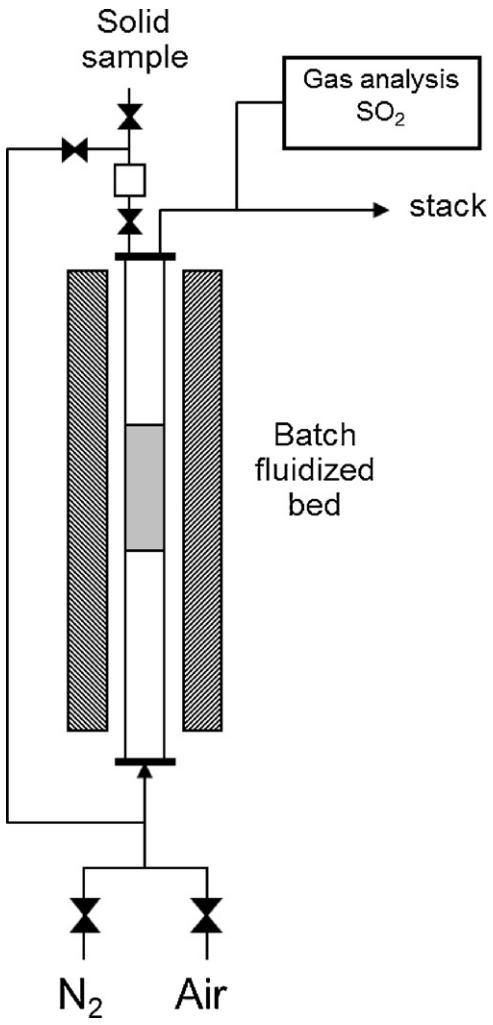

Fig. 2. Scheme of the batch fluidized bed reactor.

NiO18-αAl oxygen carrier after the operation in the CLC unit with CH_4 containing 500 vppm of H_2S, (2) to prepare samples of highly sulphided oxygen carriers, and (3) to analyse the regeneration process of the sulphided samples.

2.4. Characterization

The reducibility of the NiO18-αAl oxygen-carrier was determined by temperature-programmed reduction (TPR) experiments in a flow apparatus Micromeritics AUTOCHEM II. The sample was placed in a quartz tube and flushed with Ar during 1 h. After this pre-treatment, the oxygen-carrier particles were heated at 7 K/min from room temperature to 1323 K feeding a 20 ml/min flow of a mixture 10 vol.% H_2–90 vol.% Ar. During these tests, the accuracy in the measurements of the TPR peak was ±1 K. The amount of H_2 consumed was monitored continuously. Temperature programmed oxidation (TPO) runs were performed after cooling down the samples using 20 ml/min of a mixture 5 vol.% O_2–95 vol.% He and heating up to 1273 K at 15 K/min.

The X-ray photoelectron spectroscopy (XPS) analyses were carried out with an ESCAPlus OMICROM system equipped with a hemispherical electron energy analyser. The spectrometer was operated at 10 kV and 15 mA, using a non-monochromatized MgKα X-ray source ($h\nu$ = 1253.6 eV) and under vacuum (<5×10^{-9} Torr). Analyser pass energy of 50 eV was used for survey scans and 20 eV for detailed scans. Binding energies (BE) are referenced to the C 1s peak (284.5 eV) from adventitious carbonaceous contamination. A survey scan (1 sweep/200 ms dwell) was acquired between 1100 and 0 eV. Current region sweeps for Ni 2p, O 1s, C 1s, Al 2p and S 2p were obtained. The CASA XPS data processing software allowed smoothing, Shirley type background subtraction, peak fitting and quantification.

3. Results and discussion

3.1. Sulphur distribution in a 500 W_{th} CLC continuous unit

In a previous work [26], tests carried out in a 500 W_{th} CLC continuous pilot plant allowed studying the behaviour of the NiO18-αAl oxygen-carrier during the combustion of CH_4 (30 vol.%) in the presence of H_2S. Sulphur content in the oxygen-carrier particles extracted from the unit was too low to determine the sulphur compounds (sulphides and/or sulphates) present in the samples by usual characterization techniques. For this reason, new experiments were carried out in the CLC plant with a high concentration of H_2S for a long time trying to avoid the total regeneration of the oxygen-carrier. In this way, the sulphur content in the particles should be higher than in the previous tests and subsequent analyses would be easier.

3.1.1. Preparation of the sulphur-containing materials

In this work, new combustion tests were performed in the 500 W_{th} CLC continuous unit with 30 vol.% of CH_4 as fuel for three consecutive days. The operating temperatures were 1143 and 1223 K in the fuel and the air-reactor, respectively. The first day experiment corresponded to the reference test without H_2S. 500 vppm of H_2S were fed to the system together with the CH_4 for 11 h during the last two days. The gas velocity at the inlet of the fuel-reactor and air-reactor were 0.1 m/s and 0.45 m/s, respectively. The solids circulation rate was fixed at 12 kg/h.

Fig. 3 shows the temperature profiles in both reactors and the riser and the gas concentration at the outlet stream of the fuel and air-reactors during the third day of experimentation. CH_4 was fed to the system when the temperature reached the desired value to ensure a good performance of the unit before adding H_2S. At the beginning, some CH_4 was detected due to the formation of nickel sulphides or sulphates in the oxygen-carrier during the second day test. Nevertheless, this concentration decreased with time while CO_2 increased until reaching the steady state conditions. The oxygen-carrier seemed to recover the initial combustion capacity observed the first day of experimentation feeding only CH_4. Second peak of CH_4 was due to a solids circulation problem in the prototype. After H_2S feeding, CO_2 concentration decreased and some unburnt CH_4 appeared, while the CO and H_2 concentrations increased slowly up to 1.5 and 3 vol.%, respectively. H_2S and SO_2 were found at very low concentrations (<10 vppm) in the fuel-reactor outlet stream. SO_2 was mainly released from the air-reactor and its concentration increased with time. A sulphur mass balance in the system and the reactivity loss of the oxygen-carrier seen after introduction of H_2S started, indicated that part of the sulphur was being accumulated in the oxygen-carrier. These results were completely reproducible compared with the values obtained by Garcia-Labiano et al. [26] working with the same oxygen-carrier, NiO18-αAl.

After the operation, the solid was carefully extracted from each part of the CLC unit (air-reactor, fuel-reactor and riser) without mixing and was reserved for later tests in the batch fluidized-bed reactor.

3.1.2. Sulphur distribution in the oxygen-carrier particles after the operation

The loss of reactivity of the oxygen-carrier observed during the tests in the 500 W_{th} CLC unit was attributed to the formation

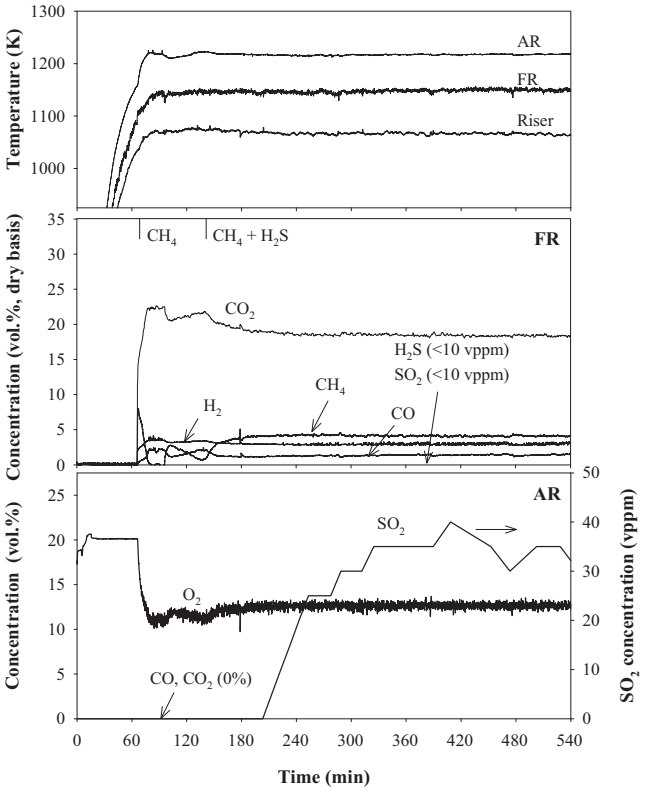

Fig. 3. Temperature and gas concentration profiles during an experiment in the 500 W_{th} CLC continuous pilot plant. CH_4 = 30 vol.%, H_2S = 500 vppm, T_{FR} = 1143 K, T_{AR} = 1223 K, G_s = 12 kg/h.

in the solid particles of some sulphur compounds like Ni_3S_2 and $NiSO_4$. To determine and to quantify the presence of these compounds in the solid after operation, 150 g samples were taken from the material extracted from the fuel-reactor, the air-reactor or the riser. These batches were heated in a batch fluidized bed reactor described above from room temperature to 1223 K in air or inert atmosphere (N_2). After that, the gas atmosphere was changed to nitrogen or air, respectively. SO_2 released in the outlet stream was continuously analysed in a non-dispersive infrared analyser (NDIR) Siemens ULTRAMAT U22.

Fig. 4 shows the SO_2 concentration emitted from the samples extracted from the fuel-reactor, the air-reactor and the riser of the CLC unit during the different steps with nitrogen and air. Each peak was attributed to one of reactions involving sulphur-containing compounds, sulphides and sulphates, shown below.

Air atmosphere:

$$Ni_3S_2 + (7/2)O_2 \rightarrow 3NiO + 2SO_2 \quad (1)$$

$$Ni_3S_2 + (9/2)O_2 \rightarrow 2NiSO_4 + NiO \quad (2)$$

Nitrogen atmosphere:

$$NiSO_4 \rightarrow NiO + SO_2 + (1/2)O_2 \quad (3)$$

$$Ni_3S_2 + 7NiSO_4 \rightarrow 10NiO + 9SO_2 \quad (4)$$

First the results obtained during the heating in air were considered. Nickel sulphide present in the samples could be oxidized directly to NiO and SO_2 at high temperatures and cause the release of SO_2 according to reaction (1). The only SO_2 peak detected at 1170 K during the heating of the samples from the fuel-reactor, air-reactor and riser could be assigned to this reaction. In addition, nickel sulphide could be also oxidized to $NiSO_4$ through reaction (2), without any SO_2 release. To demonstrate this hypothesis, air was switched to N_2 and SO_2 was released again from the reactor. This peak would correspond to the decomposition of the nickel sulphate (reaction (3)), either already present in the initial sample or formed in the previous oxidation step.

When the samples were heated up in N_2, two SO_2 peaks were observed at ≈600 K and ≈1200 K. Thermodynamic calculations using HSC Chemistry software [29] showed that Ni_3S_2 could not decompose in this inert atmosphere, so the gaseous SO_2 only could come from reactions involving $NiSO_4$. The peak at high temperature could be attributed to the decomposition of this compound to give NiO and SO_2 by reaction (3). At low temperatures, both sulphur-containing compounds can react according reaction (4) to release SO_2. Further changes of gas atmosphere produced similar results to the ones explained above during the tests heating in air.

Assuming that the proposed reactions (1)–(4) took place in the system, the integration of the different peaks shown in Fig. 4 gave us the distribution of the sulphur between Ni_3S_2 and $NiSO_4$ in the samples, as well as an approximation of the total sulphur released at those conditions. These data are summarized in Table 2. Ni_3S_2 was the major sulphur compound in the sample extracted from the fuel-reactor although some small amounts of $NiSO_4$ remained in the particles. On the contrary, $NiSO_4$ was the major sulphur compound in the samples extracted from the air-reactor with small contribution of the Ni_3S_2. Part of the sulphur retained in the solid as nickel sulphide in the fuel-reactor was released as SO_2 in the air-reactor during the operation in the CLC continuous plant. For this reason, the sulphur amount in the air-reactor sample was lower. This agreed with the results shown in the previous work by Garcia-Labiano et al. [26].

The SO_2 concentration curves of oxygen-carrier from the riser should be the same as the ones obtained with the solid from the air-reactor. Nevertheless, as can be seen in Table 2 and Fig. 4, slight differences were observed during the heating in N_2 as well as in air. The SO_2 peaks from $NiSO_4$ decomposition increased their intensity. This seemed to indicate that the lower temperature in the riser with respect to the air-reactor favoured the formation of $NiSO_4$ from the reaction between gaseous SO_2 and NiO in the oxidized oxygen-carrier through the reverse reaction (3). This fact confirmed the formation of sulphur compounds in the riser proposed by Garcia-Labiano et al. [26]. Lower temperatures in the riser were due to the specific design of this CLC plant. Nevertheless, formation of $NiSO_4$ could be avoided in an industrial scale CLC plant working at higher temperatures in the riser.

In any case, the above tests and the subsequent sulphur balance showed that part of the sulphur present in the samples remained inside the particles despite of the successive regeneration steps with nitrogen or air. Approximately 50% of the sulphur fed to the 500 W_{th} CLC was not emitted as SO_2 or H_2S in either the fuel- or the air-reactor and it was not eliminated during the tests in the batch fluidized bed reactor. It must be considered that the desired situation during the operation of an industrial scale CLC plant would be the emission of all the sulphur contained in the fuel as SO_2 in the air-reactor. This will allow having a fully regenerated and highly reactive oxygen-carrier at the fuel-reactor inlet. To analyse this possibility, new experiments were planned in the batch fluidized bed reactor to study the influence of different parameters (temperature

Table 2
Sulphur distribution in the oxygen-carrier samples extracted from the CLC continuous unit after CH_4 combustion experiments in the presence of H_2S.

	Sulphur in the sample (mg S/100 g sample)	Sulphur distribution (%)[a]	
		Ni_3S_2	$NiSO_4$
Fuel-reactor	11.6	86	14
Air-reactor	5.9	16	84
Riser	11.2	17	83

[a] Inferred from SO_2 release in BFB according to reactions (1)–(4).

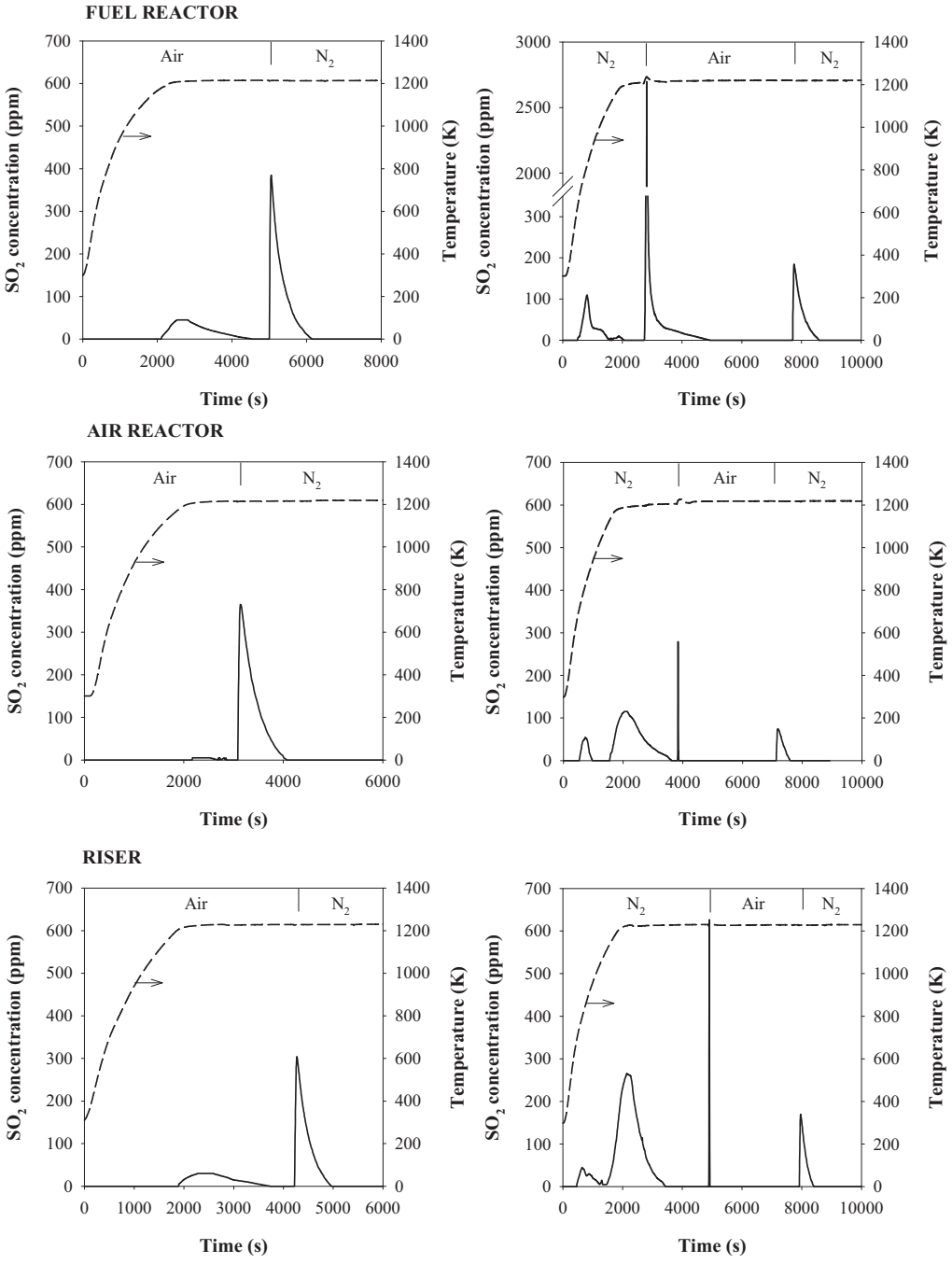

Fig. 4. SO_2 concentration released during the heating of the NiO18-αAl oxygen-carrier extracted from the fuel-reactor, air-reactor and riser in air and nitrogen atmosphere.

and oxygen concentration) in the oxygen-carrier regeneration, as explained below.

3.2. Studies about the regeneration of the oxygen-carrier

During previous combustion tests with the NiO18-αAl oxygen-carrier in the CLC continuous unit feeding mixtures CH_4–H_2S, it was observed that the SO_2 concentration in the outlet stream of the air-reactor varied depending on the air-reactor and riser temperatures [26]. To analyse the effect of the temperature and the oxygen concentration on the regeneration of the sulphur-containing oxygen-carrier, new sulphided material with high S content was prepared and several experiments at different operating conditions were carried out in the batch fluidized bed reactor.

3.2.1. Preparation of the sulphided sample in a BFB

About 400 g of NiO18-αAl particles were reduced with 25 vol.% H_2 (N_2 balance) at 1223 K for more than 1 h in the batch fluidized-bed reactor. When the H_2 concentration in the outlet stream reached the initial value, indicating that the sample was fully reduced, the system was cooled down to 873 K and 1300 vppm of H_2S in N_2 (268 l/h, 10 cm/s) were introduced into the reactor for 45 min. 5 vol.% of H_2 was fed together with H_2S to avoid the decomposition of this gas inside the pipes. These conditions favoured the formation of nickel sulphide, considering the results from previous thermodynamic analyses [26]. Outlet stream gases were analysed in a gas chromatograph (Varian 3400-CX GC) equipped with a PORAPAK-Q packed column and a sulphur-specific flame photometric detector (FPD), calibrated in the range 0–300 vppm for both

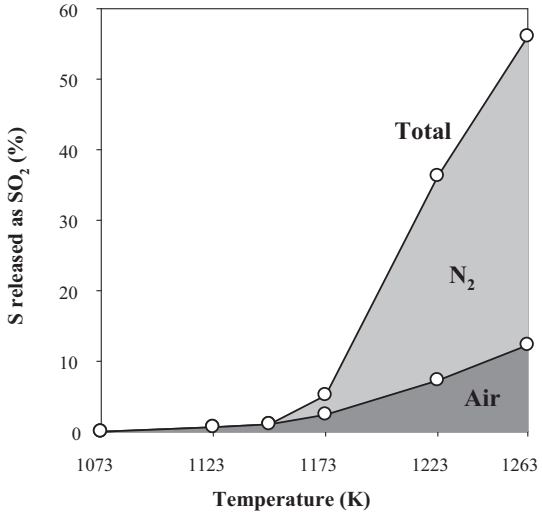

Fig. 5. Effect of temperature on the sulphur emitted as SO_2 during successive regeneration stages with air and nitrogen with sulphided samples of NiO18-αAl oxygen-carrier.

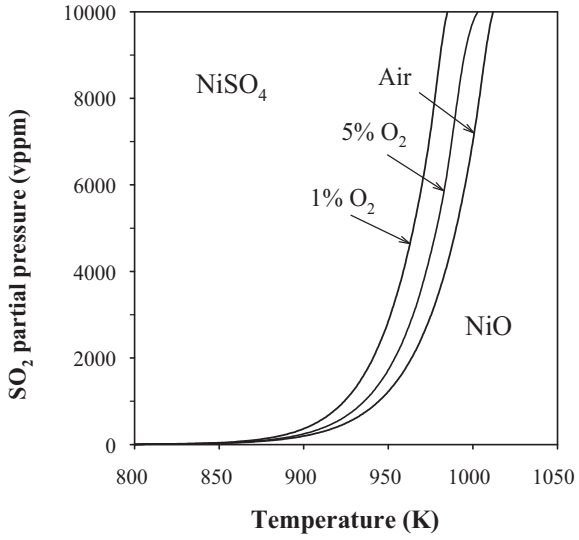

Fig. 6. Thermodynamic equilibrium for $NiSO_4$ decomposition.

H_2S and SO_2. These gases were not detected during the sulphidation process, so it could be concluded that sulphur was totally accumulated in the oxygen-carrier. The final sulphur content in the solid determined by a total sulphur analysis was 0.095 wt.%. Therefore, the conversion of Ni–Ni_3S_2 was 1.85%. Although this percentage was low, it represented a higher amount of sulphur than in the case of the samples extracted after the operation in the CLC continuous unit. The preparation process of sulphided particles (BFB-S sample) was carried out twice, so ≈800 g of NiO18-αAl oxygen-carrier were available for subsequent experiments.

3.2.2. Effect of temperature on the oxygen-carrier regeneration

The sulphided samples previously prepared were regenerated at different temperatures ranging from 1073 to 1263 K, typical temperatures of the air-reactor in a CLC plant. A bed of alumina (300–500 μm) was heated to the desired temperature and fluidized with air (190 l/h) in the batch fluidized bed reactor shown in Fig. 2. To introduce the sulphided oxygen-carrier into the reactor, a small hopper located in the upper part of the reactor was used. Then, 20 g of the sulphided particles were quickly introduced into the bed and the released SO_2 was measured continuously using a non-dispersive infrared analyser (Siemens ULTRAMAT U22). When the SO_2 concentration fell down to zero, air was replaced by N_2 trying to regenerate the oxygen-carrier particles completely. Every test was repeated twice and negligible variations among them were found.

Fig. 5 shows the sulphur emitted as SO_2 with respect to the total sulphur present in the sample using air and subsequently nitrogen as fluidization agents at different temperatures. The amount of SO_2 released at temperatures below 1173 K, according to reaction (1), was very low and most of the nickel sulphide was converted into nickel sulphate (reaction (2)). This fact can be explained attending to the thermodynamic equilibrium for $NiSO_4$ decomposition, shown in Fig. 6. Independently of the oxygen concentration and SO_2 partial pressure, decomposition started being noticeable at 900 K. Nevertheless, the reaction rate might be very low at that temperature since about 200 degrees more were necessary to observe SO_2 formation experimentally. The change from air to N_2 produced SO_2 emissions again (reactions (3) and (4)), indicating the presence of $NiSO_4$ in the sample formed during the previous air feeding step.

It must be pointed out that the oxygen-carrier was never fully regenerated at any of the temperatures tested. A maximum of 12 wt.% of the sulphur could be emitted as SO_2 at the oxidation conditions in air atmosphere. Even if the solid was later treated with nitrogen, only 56 wt.% of the sulphur would be released at 1263 K. These results indicated that the regeneration of the sulphided particles is rather difficult even at high temperatures and part of the sulphur always remains in the solid.

3.2.3. Effect of oxygen concentration on the oxygen-carrier regeneration

The effect of the oxygen concentration on the oxygen-carrier regeneration was also analysed. The experimental procedure was similar to the one described above. In this case, different O_2–N_2 mixtures were used as fluidizing agent instead air at 1223 K.

Fig. 7 shows the percentage of sulphur emitted as SO_2 when the sulphided particles were fed into the fluidized bed reactor with different O_2 concentrations. As can be observed, the SO_2 release decreased as the O_2 content in the gas fed to the reactor raised. Therefore, an important effect of the O_2 was inferred since the nickel sulphide oxidation to form nickel sulphate was favoured when the oxygen concentration was high. This fact was confirmed when the O_2–N_2 mixture was replaced by pure N_2 and the SO_2

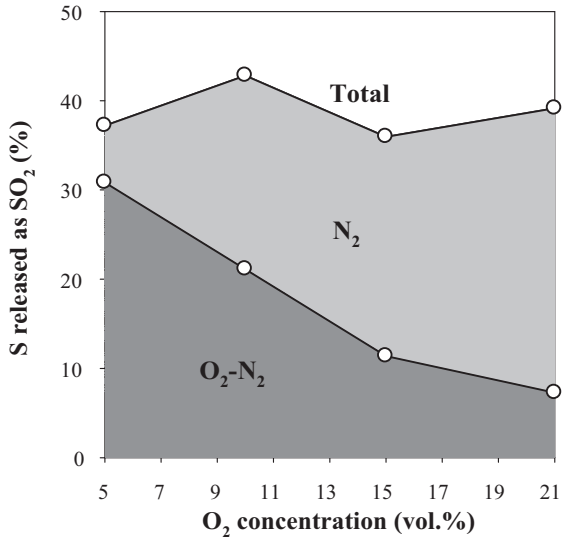

Fig. 7. Effect of oxygen concentration on the sulphur emitted as SO_2 during successive regeneration stages with O_2–N_2 mixtures and nitrogen with sulphided samples of NiO18-αAl oxygen-carrier. T = 1223 K.

release as a consequence of the $NiSO_4$ decomposition took place. It must be highlighted that only about 40 wt.% of the total sulphur present in the particles reacted with the O_2, either to release SO_2 or to form sulphates while the rest remain inside the particles.

Nevertheless, regeneration tests carried out during the experiments in the CLC pilot plant with fuel containing H_2S showed that the oxygen-carrier was capable of recovering its initial reactivity after several hours without H_2S feeding [26]. Fig. 8 shows the TGA reactivity data for the fresh (as prepared) and the regenerated oxygen-carrier after experiments with 300–1000 ppm of H_2S. As can be seen, the reactivity was very high with a solids conversion higher than 90% during the reduction and almost full conversion in the oxidation before 1 min. At these conditions, the oxygen-carrier could be used with good performance despite the remaining sulphur in the particles. Obviously, although the reactivity could be recovered, the sulphur remaining in the particles would produce a decrease in the oxygen transport capacity of the material along its life-time. To corroborate the above results a deeper analysis of the solid particles by means of different characterization techniques was performed.

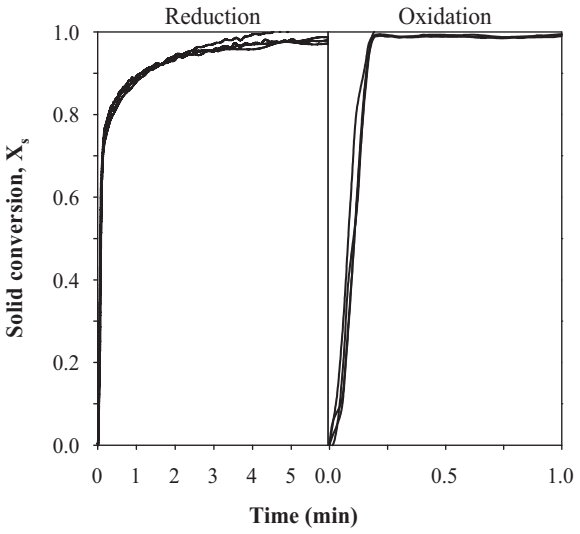

Fig. 8. TGA reactivity for the fresh and the regenerated oxygen carrier. T = 1223 K. 15 vol.% CH_4 during reduction; air during oxidation.

3.3. Characterization of the NiO18-αAl oxygen-carrier particles after their use in the presence of sulphur

According to the results shown above, full regeneration of the NiO18-αAl oxygen-carrier would not be possible at the selected conditions of temperature and oxygen concentration. The interaction of the sulphur with the complex structure of the oxygen-carrier containing different Ni and Al compounds (NiO, $NiAl_2O_4$, α-Al_2O_3, etc.) could affect the regeneration process. TPR–TPO and XPS analysis were carried out to analyse the reducibility and to characterize the surface of the oxygen-carrier particles, identifying the main elements, their oxidation state and the type of chemical structure.

Several samples extracted from the CLC continuous unit, before and after the operation with H_2S, and from the BFB reactor,

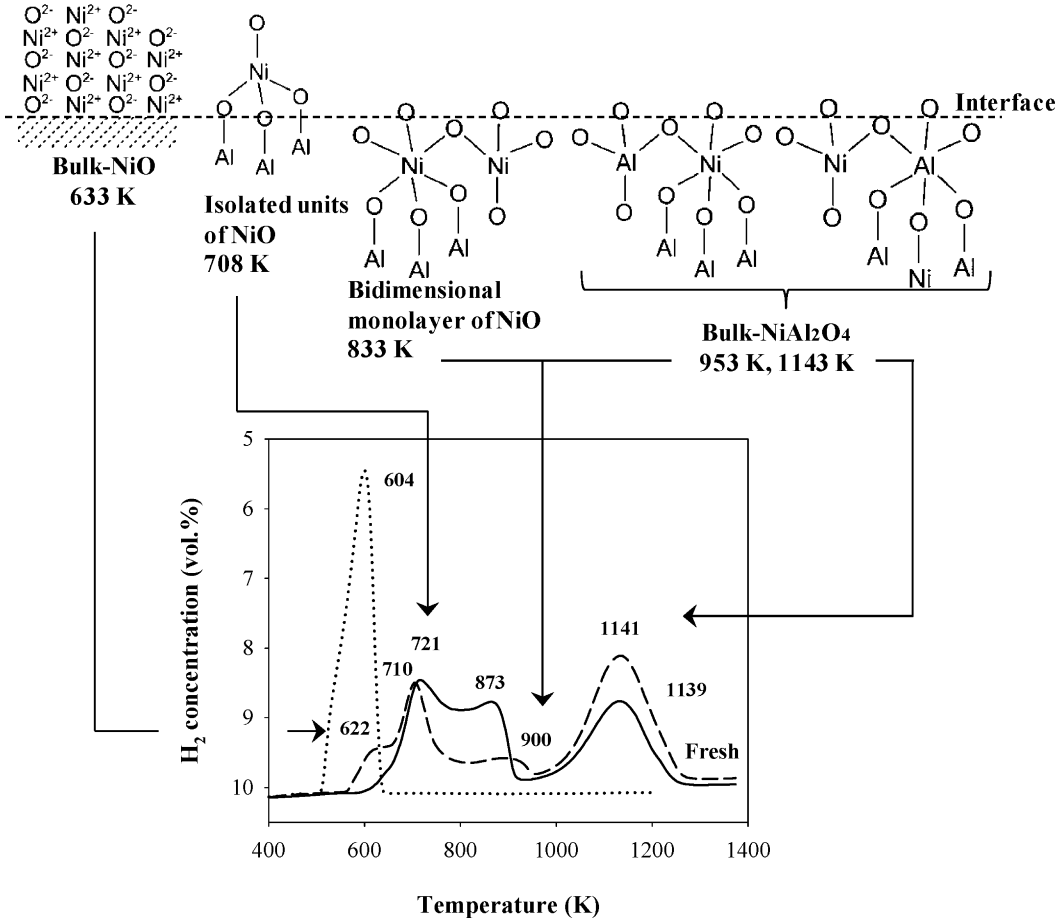

Fig. 9. TPR profile of the fresh NiO18-αAl oxygen-carrier (–) and after a TPO run (- - -). Theoretical temperature values of the different structures obtained from references [30–33]. TPR of pure NiO is shown as reference (· · ·).

Table 3
Position of the peaks and bands in TPR analysis. Data in K.

Sample	TPR-1	TPR-2[a]
Fresh	721, 873, 1139	622, 710, 900, 1141
CLC	647, 683, 763, 1217	620, 705, 1078
CLC-S(FR)	583, 658, 833, 1116	626, 700, 875, 1133
CLC-S(AR)	689, 735, 1135	629, 721, 1086
BFB-S	555	555
BFB-R(A)	719, 821, 1162	729, 853, 922, 1123
BFB-R(AN)	711, 803, 1185	722, 856, 1167

[a] After a TPO run.

sulphided and regenerated, were considered for the characterization. The study of fresh oxygen-carrier (so-called Fresh) and particles extracted from the CLC unit after 7 h of combustion with CH_4 but without H_2S (sample CLC) were considered as reference. Two sulphur-containing samples extracted from the fuel-reactor -CLC-S(FR)- and the air-reactor -CLC-S(AR)- after the operation with H_2S feeding in the CLC unit were used for further analysis.

Three different samples were selected to investigate the solid from the batch fluidized bed reactor: the original sulphided oxygen-carrier prepared as explained above (BFB-S), the sulphided oxygen-carrier after a regeneration step with air -BFB-R(A)-, and the material regenerated with air and N_2 at 1223 K -BFB-R(AN)-.

3.3.1. Temperature-programmed reduction (TPR)

Pure NiO (Sigma–Aldrich Chemie GmbH, Germany, Nickel (II) oxide, black, <10 μm) and α-Al_2O_3, prepared by calcination of commercial γ-Al_2O_3 (Puralox NWa 155, Sasol Germany GmbH, 100–300 μm) were used as reference materials for TPR tests. The TPR curve of pure NiO powder showed a single peak of hydrogen consumption with a maximum at 604 K, as can be seen in Fig. 9. As expected, an almost negligible peak of hydrogen consumption was observed at 601 K for α-Al_2O_3.

Hydrogen consumption peaks during the TPR analysis of the fresh NiO18-αAl oxygen-carrier are shown in Fig. 9. These fresh particles exhibited three peaks of hydrogen consumption whose positions and bands are reported in Table 3. This could be due to the presence of different NiO species on the alumina and agreed with several studies in literature [30–33]. First peak (≈721 K) could be attributed to isolated NiO units on the surface of the support. The interaction with the alumina was weak but enough to need a higher temperature to be reduced than the one corresponding to bulk NiO. Second peak (≈873 K) was related to the presence of a bi-dimensional NiO monolayer on the top of the support with moderate interaction with α-Al_2O_3. Finally, the third peak (≈1139 K) corresponded to a strong interaction with the support. Either nickel species incorporated in the surface of the support having nickel aluminate character or bulk-$NiAl_2O_4$ consisting of nickel cations which migrated deeply under the surface of the alumina support appeared.

After a TPO experiment, a new TPR profile was obtained. Some differences with respect to the first analysis were observed, such as a shoulder around 622 K. This could reflect the reduction of Ni^{3+} (oxygen excess after TPO) according to the above mentioned literature [31–34]. Moreover, the second hydrogen consumption peak, corresponding to isolated units of NiO, shifted to lower temperatures. After the oxidation, the interaction with the support decreased slightly and therefore the reduction of the sample was easier. The peak at 873 K almost disappeared and shifted to around 900 K. This was related to the successive reduction of nickel ions of octahedral and tetrahedral symmetry from non-stoichiometric surface nickel aluminate. The peak corresponding to nickel aluminate appeared at the same temperature but the amount of hydrogen consumption increased significantly. The successive reduction of nickel ions between the two symmetries could explain this fact [34].

A TPR analysis of the samples extracted from the CLC continuous pilot plant was also carried out (TPR-1), as can be seen in Fig. 10. The position of peaks and bands are summarized in Table 3. Significant differences were found regarding the TPR of the fresh NiO18-αAl oxygen-carrier. Most of the nickel was present as nickel aluminate in the samples from both the fuel- and the air-reactor, in contrast with the fresh oxygen-carrier that had a higher content of free NiO. At the same time, the NiO peak was much lower and its asymmetry indicated a contribution of bulk and isolated NiO species showing a weak interaction with the α-Al_2O_3 support. These results agreed with a previous work carried out by Dueso et al. [35] where the ratio NiO/$NiAl_2O_4$ in the particles was not a constant but a function of the reduction conversion during the previous redox cycles.

After the in situ oxidation (TPO) of the samples, a second TPR was performed (TPR-2). At these conditions, almost all the nickel aluminate was converted to NiO during the oxidation of the samples extracted from the air-reactor (CLC and CLC-S(AR)). These results were directly related to those observed in the study of the NiO18-αAl oxygen-carrier reactivity [35]. Sulphur accumulated in the solid particles did not seem to affect the reducibility behaviour of the CLC-S(AR) sample. Nevertheless, the sample extracted from the fuel-reactor (CLC-S(FR)) exhibited a different pattern than the above solid. In this case, an important amount of nickel aluminate was maintained, likely due to the higher content of Ni_3S_2 and $NiSO_4$ in this sample than in the one obtained from the air-reactor, where the oxygen-carrier was partially regenerated. Ni could have migrated to deeper layers of bulk-$NiAl_2O_4$ to form the nickel sulphide and sulphate, being more difficult to convert into NiO. Further XPS analysis shown below could explain this fact.

The TPR profiles of the samples coming from the batch experiments -BFB-S, BFB-R(AN) and BFB-R(A)- are depicted in Fig. 11. These samples TPR profiles were quite different from those exhibited by the samples extracted from the CLC plant (Fig. 8). TPR profiles of BFB-R(A) and BFB-R(AN) were very similar to that corresponding to the fresh sample, indicating that the regeneration with air or air/N_2 of the sulphided samples did not alter significantly the Ni species distribution. However, the TPR profile of these two samples obtained after a TPO run (TPR-2) underwent a change. The sample oxidized with air, BFB-R(A), suffered a high re-dispersion of the active phase and the peak corresponding to nickel aluminate almost disappeared, in a similar way to the samples CLC and CLC-S(AR). Nevertheless, the peak of nickel aluminate for the sample exposed to consecutive stages of oxidation with air and N_2 (BFB-R(AN)) was not altered after reoxidation. The only redistribution of the active phase observed took place between NiO species with different interaction strength with the support. This could be also related with the different amounts of sulphur present in both regenerated samples.

The sulphided NiO18-αAl particles (BFB-S) had a different behaviour with respect to the rest of the samples from both the CLC pilot plant and the batch fluidized bed reactor. A peak with a branch starting at ≈633 K appeared at 555 K. A similar form of the TPR curve was reported by Kuhn et al. [36] for Ni-YSZ treated with H_2S. However, after the in situ oxidation, TPR profile was quite similar to the one obtained with the sample BFB-R(AN), indicating some reversibility of the sulphidation process.

In order to explain the behaviour of the BFB-S particles and for comparison purposes, a TPR experiment was carried out with a mixture of 1 wt.% commercial nickel sulphide (Ni_3S_2 Aldrich, 99.7% trace metals basis, −150 mesh) with the same α-Al_2O_3 used to prepare the NiO18-αAl oxygen-carrier. As can be seen in Fig. 12, no peaks were detected for the Ni_3S_2/α-Al_2O_3 mixture and only a branch starting around 628 K, similar to that exhibited by the sample BFB-S, was observed. Thus, the form of the TPR profile for the

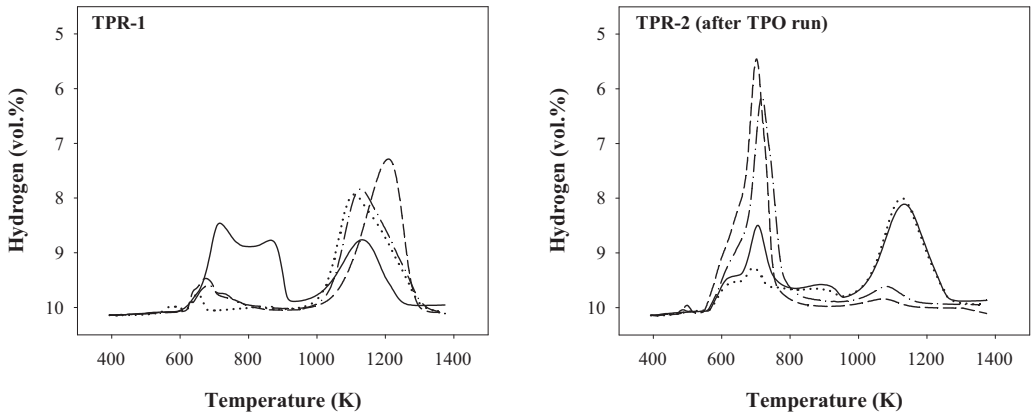

Fig. 10. TPR profiles of the samples extracted from the CLC continuous pilot plant burning a fuel containing sulphur: (–) Fresh oxygen-carrier, (- - -) CLC, (-·-·-) CLC-S(AR) and (···) CLC-S (FR).

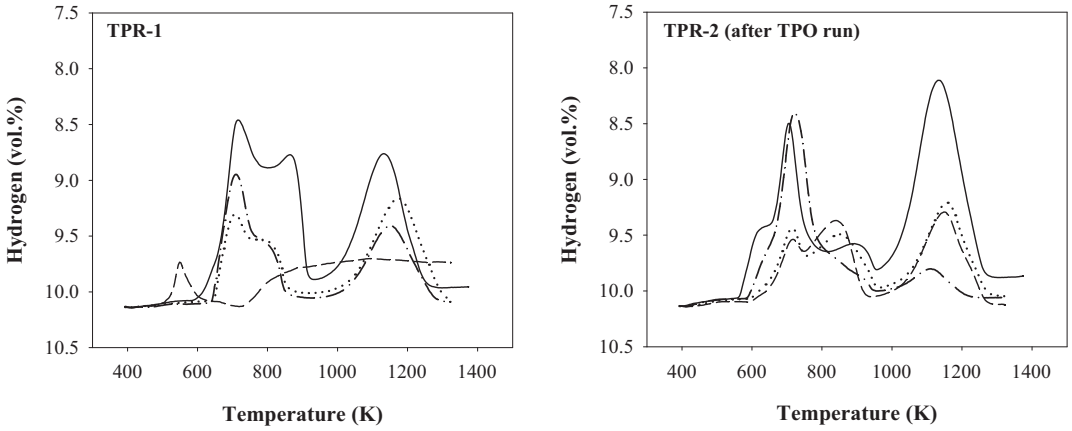

Fig. 11. TPR profiles of the samples prepared in the BFB reactor: (–) fresh oxygen-carrier, (—·) sulphided particles BFB-S, (-·-·-) after regeneration with air BFB-R(A) and (···) after regeneration with air and N_2, BFB-R (AN).

BFB-S sample could be explained in the same terms. In addition, the small peak at 555 K could be attributed to the presence of some NiS_2 in the sample, the less stable sulphide, as proposed by Afanasiev [37]. It must be considered that the operating conditions during the preparation of the BFB-S sample were quite different from the conditions existing in the fuel-reactor of the CLC unit where full reduction of the materials is never reached. The lack of conclusive evidences for this hypothesis by TPR analyses could be clarified by the following XPS analyses.

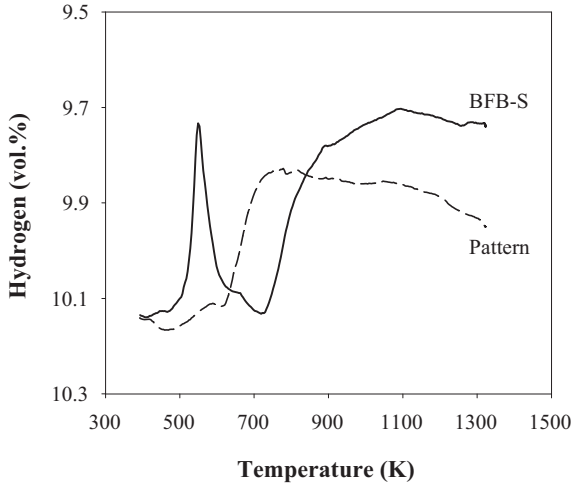

Fig. 12. TPR profiles of the sulphided NiO18-αAl oxygen-carrier (BFB-S) and the pattern sample (1 wt.% Ni_3S_2/α-Al_2O_3).

3.3.2. X-ray photoelectron spectroscopy (XPS)

Binding energy regimes containing the Ni 2p and S 2p emission lines of the samples extracted from the CLC continuous plant are shown in Fig. 13. The position of the Ni $2p_{3/2}$ line varied from 855.4 to 855.6 eV. For these samples the position of the Ni $2p_{1/2}$ line was found at 17.9 eV higher binding energy in comparison to Ni $2p_{3/2}$ line. For both emission lines a shake-up satellite was found with a binding energy about 6.2–6.0 eV higher. The position of the Ni $2p_{3/2}$ line around 855.5 eV with the associated satellite indicated the presence of one or more nickel–oxygen species. The fitting of the peaks showed the presence of several contributions

Table 4
Surface analysis from XPS spectra.

Sample	Ni 2p region BE (eV)			S 2p region BE (eV)		
CLC	853.6	855.6				
CLC-S(FR)	853.2	855.5	856.7	160.5	163.1	168.5
CLC-S(AR)	852.6	855.4	856.6	160.0	163.2	168.5
BFB-S	854.3			161.6	162.8	169.1
BFB-S[a]	851.9			160.7	162.7	
BFB-R(AN)	854.0	855.7		161.0	162.6	167.6
BFB-R(AN)[a]	851.8	852.6	855.6	160.5	163.3	167.4

[a] After sputtering.

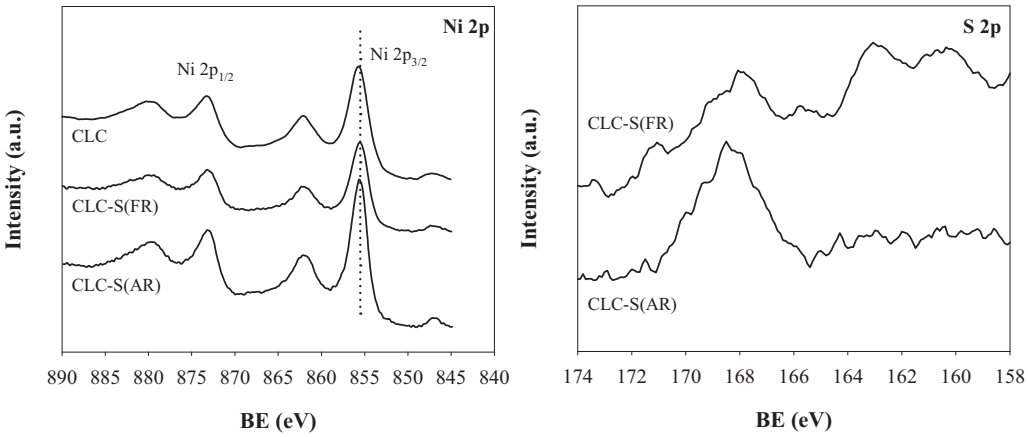

Fig. 13. XPS surface spectra for Ni 2p and S 2p of the samples extracted from the CLC continuous pilot plant during combustion tests with CH_4 containing H_2S as fuel.

whose BEs are given in Table 4. As an example, Fig. 14 shows the fitting of the peaks found for the CLC-S(FR) sample. These BEs could be assigned to different Ni or S compounds according to data available in literature [36,38–40].

Regarding to nickel peaks, sample CLC exhibited two contributions. The first one was attributed to the presence of Ni^{2+} in octahedral sites in the form of NiO showing a weak interaction with the support whereas the second peak could be ascribed to Ni^{2+} in the tetrahedral position of a spinel-like structure such as $NiAl_2O_4$. This analysis confirmed the distribution of the impregnated nickel in the NiO18-αAl oxygen-carrier between bulk nickel oxide, easy to reduce owing to a low interaction with the α-Al_2O_3 support, and $NiAl_2O_4$, formed from the reaction between free NiO and the alumina support at high temperatures, as found in previous works [23,27,35] and in the preceding TPR analysis (Fig. 10).

For the sulphur-containing samples CLC-S(FR) and CLC-S(AR), the first peak in the Ni 2p region shifted to a lower BE (Table 4), near to the one corresponding to Ni^0. Nevertheless, the satellite peak is almost unaltered. Therefore, the presence of NiS instead of Ni^0 was considered. Mangnus et al. [41] found that NiS is the preferred sulphide when the content of nickel over an alumina support is high. It is known that strong metal-support interactions give rise to the appearance of NiS whilst Ni_3S_2 is preferentially found in systems with weak metal-support interactions [42]. This could be the case of the NiO18-αAl oxygen-carrier, with a very high content of nickel in comparison with the amount of sulphur in the solid particles and a strong interaction of the metal with the support to form $NiAl_2O_4$. However, curve fitting of Ni $2p_{3/2}$ emission line gave a very small contribution of this sulphide. The second peak of the XPS spectra around 855.5 eV remained almost unchanged in both samples, which means that part of Ni^{2+} was in the form of $NiAl_2O_4$, as in the case of the CLC sample without sulphur. This indicates that sulphur mainly reacts with nickel in the form of NiO.

However, the most relevant result obtained with these sulphur-containing samples was the new peak found in the deconvolution of the Ni $2p_{3/2}$ region. This peak at about 857 eV could be attributed to either Ni_3S_2 phase, according to the Ni_3S_2 standard in Kuhn et al. [36], or to sulphur–oxygen species. Arnoldy et al. [43] proposed a sulphidation mechanism of oxidic nickel catalysts by H_2S through O–S exchange.

To get an insight into the species found on the different samples, XPS of the S 2p region was obtained and analysed. These results should be consistent with the Ni $2p_{3/2}$ XPS results showed above. The position of the fitted peaks is presented in Table 4. A peak and two broad bands of lower intensity were observed for the sample CLC-S(AR). The peak in the range 166–169 eV indicates the presence of Ni–O–S species according to previously cited literature [36,40]. Based on Buckley and Woods [40], the two bands could correspond to the doublet exhibited by the XPS pattern of Ni_3S_2 standard. However, after curve fitting of the S 2p emission line, the separation of the BEs found for these samples was higher than that found for the standard sulphide. Moreover, the intensity and the area of the high BE contribution of the doublet found for the standard was lower than those for the low BE contribution. This could be due to the presence of other Ni–S species, such as NiS. These findings agreed with the conclusions made from the analysis of the Ni $2p_{3/2}$ region,

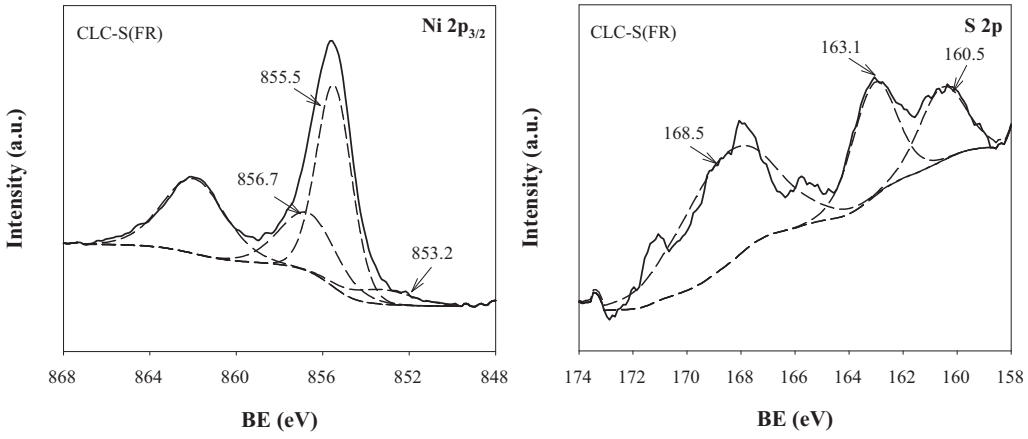

Fig. 14. Deconvolution of the XPS peaks of CLC-S(FR) sample in the Ni $2p_{3/2}$ and S 2p regions.

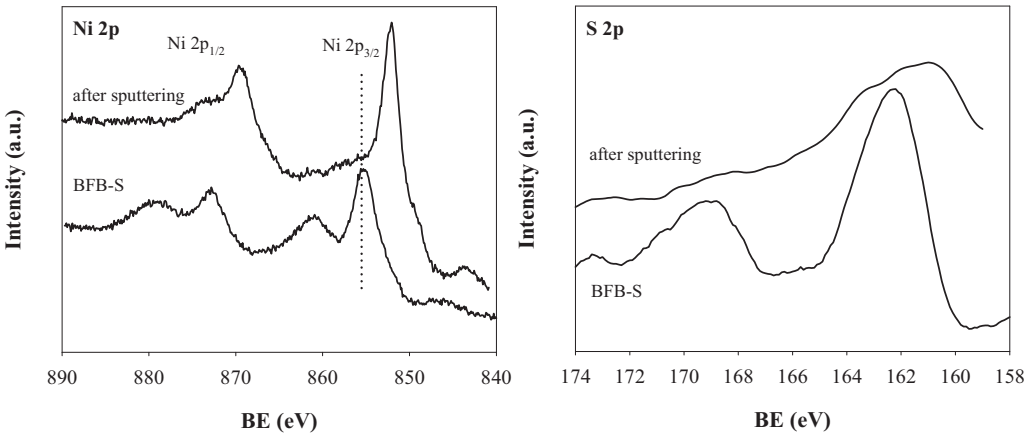

Fig. 15. XPS surface spectra for Ni 2p and S 2p of sulphided sample prepared in the batch fluidized bed reactor, BFB-S.

which suggested the presence of this sulphur compound in small amounts together with the major Ni_3S_2.

The sample CLC-S(FR) extracted from the fuel-reactor of the 500 W_{th} CLC unit plant showed a slightly different spectrum than that of the sample from the air-reactor. The intensity of the bands of the nickel sulphides was higher while the intensity of the peak attributed to Ni–O–S species was lower. Hence, the proposed formation of nickel sulphide in the oxygen-carrier particles during the combustion of CH_4 in the presence of H_2S inside the fuel-reactor [26] was confirmed. It must be also remarked the presence of Ni–O–S species in the samples from the fuel-reactor, which could be related with sulphate compounds.

The XPS spectra of the BFB reactor samples are shown in Fig. 15. Sulphided sample (BFB-S) showed a Ni 2p XPS pattern similar to those of the samples extracted from the CLC continuous plant (see Fig. 13), although the TPR profiles were very different. An XRD analysis of these samples confirmed the presence of metallic nickel, coming from the almost complete reduction of the sample during the sulphidation stage in the BFB reactor, and α-Al_2O_3. However, the Ni $2p_{3/2}$ line surprisingly appeared at 854.3 eV and the shake-up satellite indicated the presence of divalent species. On the other hand, line S 2p showed two wide peaks. First peak was found at 162.2 eV and corresponded to Ni_3S_2 phase. The curve fitting of this peak gave the expected doublet for Ni_3S_2 (161.6 and 162.8 eV). The selected operating conditions for the preparation (873 K, 1300 vppm of H_2S) favoured the formation of a stable nickel sulphide as expected. The second band had the maximum at 169.1 eV, typical for Ni–O–S species. This finding was also quite surprising because the conditions in the BFB reactor were reducing instead oxidizing so this kind of compounds should not be observed. In this case, a possible oxidation during sample manipulation could be inferred. To confirm that, an analysis of the composition of the inner part of the particles was carried out. The BFB-S sample was sputtered in situ at the same conditions previously reported. The Ni 2p and S 2p XPS lines can be seen in Fig. 15. The Ni $2p_{3/2}$ line shifted to a binding energy corresponding to metallic nickel and the satellite peak shrunk almost completely, indicating that divalent Ni species had almost disappeared. S 2p line showed only one peak related to Ni_3S_2 phase. However, the concentration of this compound was very low because the intensity of the peak decreased with respect to the analysis of the surface. The peak at higher BE assigned to Ni–O–S species disappeared. Therefore, only the surface of the particles was oxidized. At this high BE only a shoulder corresponding to Ni_3S_2 phase was found [36]. These results demonstrated that the nickel sulphide is formed preferably in the surface of the particles, easily oxidized.

Finally, the sample regenerated in two stages with air and N_2 (BFB-R(AN)) was analysed (Fig. 16). The XPS spectrum of Ni $2p_{3/2}$ region showed one peak with two contributions: the first one could be attributed to Ni^{2+} in octahedral sites as NiO with weak interaction with the support and the second peak could be assigned to Ni^{2+} in tetrahedral position of a spinel-like structure as $NiAl_2O_4$. As it has been previously mentioned, nickel inside NiO18-αAl particles was distributed between free NiO and $NiAl_2O_4$. So these results agreed with the previous TPR analysis. Despite the regeneration treatment, the S 2p region also showed the presence of sulphur

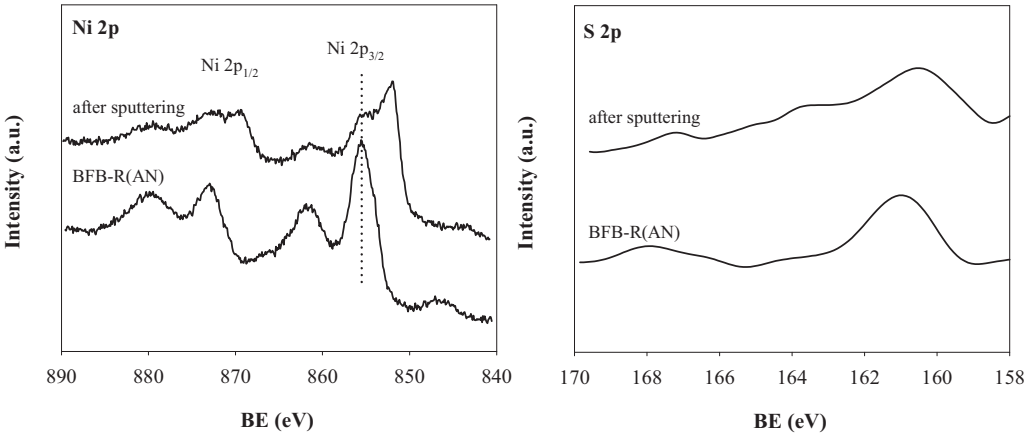

Fig. 16. XPS surface spectra for Ni 2p and S 2p of regenerated sample prepared in the batch fluidized bed reactor, BFB-R (AN).

compounds on the surface of the carrier, although twice less intense than the one corresponding to the BFB-S sample. The main contributions were assigned to Ni_3S_2 phase and Ni–O–S species. The corresponding species could not be followed in the Ni $2p_{3/2}$ region due to the low intensity of the contribution of nickel sulphide to Ni $2p_{3/2}$ peak compared to the intensity of the contribution of NiO and $NiAl_2O_4$ species. In order to determine the evolution of sulphur inside the particles, the sample was also sputtered with an Ar ion gun. Ni $2p_{3/2}$ peak after sputtering shifted to lower binding energies and the presence of different contributions was evident from the pattern. The satellite shrunk near 20%, indicating the presence of metallic nickel in some extent. This result could not be followed by TPR technique, because of the reasons mentioned above. The intensity of the S 2p peak after sputtering was near twice lower than that corresponding to the received sample and Ni–O–S species almost disappeared, being these results similar than those found for the BFB-S sample.

Although quantifying is difficult using XPS technique, the intensity of the peaks in both samples (as received and after sputtering) indicated that about 1/3 of the sulphur present in the sample remain inside the particle, mostly in the form of nickel sulphide. This result agrees with the found in the regeneration tests carried out in the BFB at different temperatures and oxygen concentrations, where the presence of sulphur inside the samples was also inferred.

Therefore, it can be concluded that the complete regeneration of the oxygen-carriers during oxidation in the air-reactor was not possible, and sulphur was being continuously accumulating inside the particles. A previous desulphurization step of the fuel would be necessary before using it in a CLC plant if Ni-based oxygen-carriers are going to be used. In any case, it must be mentioned that regenerated particles, even containing some sulphur inside, were able to maintain the reactivity regarding CH_4 combustion reaction.

4. Conclusions

Gaseous fuels for chemical-looping combustion (CLC) process could contain sulphur-compounds which affect the oxygen-carrier behaviour, especially if NiO is used as active phase. The loss of reactivity when NiO18-αAl oxygen-carrier was used in a CLC continuous unit with CH_4 containing H_2S as fuel was attributed to the formation of nickel sulphides and sulphates. In this work the distribution of the sulphur in the solid particles extracted from each part of the plant after the operation (CH_4 + 500 vppm H_2S for 11 h) was determined from a heating up process in a fluidized bed reactor in nitrogen or air atmosphere. 86% of the sulphur in the particles from the fuel-reactor was in the form of Ni_3S_2 while 14% corresponded to $NiSO_4$. The amount of sulphur in the air-reactor was reduced to almost a half and the ratio Ni_3S_2–$NiSO_4$ was reversed (16–84). Although the oxygen-carrier recovered from the riser kept the proportions between both sulphur compounds with respect to the sample of the air-reactor, the amount of sulphur increased almost to the levels in the fuel-reactor. Lower temperatures in this part of the unit could favour the reaction of the gaseous SO_2 formed in the air-reactor with the NiO in the solid particles although this particularity of our installation should not occurred at industrial scale.

A regeneration study of the oxygen-carrier was also performed in order to determine the optimal situation to emit as much sulphur as possible in the air-reactor avoiding the accumulation in the particles. Additional tests with a sulphided NiO18-αAl oxygen-carrier (0.095 wt.%) previously prepared were carried out in a batch fluidized bed reactor at different temperatures (1073–1263 K) and oxygen concentrations (0–21 vol.%). Independently of the operating conditions, part of the sulphur remained in the solid and total regeneration was not possible. Nevertheless, the oxygen-carrier seemed to reach its initial reactivity after a regeneration step, so the remaining sulphur did not affect the behaviour of the oxygen-carrier regarding CH_4 combustion, although the oxygen transport capacity was decreased through the operation time.

The analysis of the NiO18-αAl oxygen-carrier samples using TPR and XPS techniques revealed that the sulphur reacted preferably with free NiO instead of $NiAl_2O_4$. Ni_3S_2 was found to be the major sulphide in the samples obtained after the operation in the 500 W_{th} CLC unit although minor amounts of NiS were also detected. Sulphur was preferably concentrated in the outer surface of the particles. TPR analysis showed that sulphur accumulated in the oxygen-carrier did not affect the reducibility behaviour. The sulphidation and later stages of oxidation with air and N_2 or only air did not alter significantly the Ni species distribution between NiO and $NiAl_2O_4$. Nevertheless, the presence of a low S 2p peak in the XPS analysis of the regenerated samples of sulphided NiO18-αAl oxygen-carrier indicated that total regeneration of the particles after their use with H_2S did not take place. Taking into account all the results found, a previous desulphuration process of the fuel would be necessary when using NiO-based oxygen-carriers in the CLC system.

Acknowledgements

This research was conducted with financial support from the European Commission, under the Sixth Framework Program, Contract no. 019800-CLC GAS POWER, by the CCP2 (CO_2 Capture Project), a partnership of BP, Chevron, Conoco-Phillips, Eni Technology, Norsk Hydro, Shell, Suncor and Petrobras. The authors thank I. Fernández, N. Fernández and E. Ayllón their help with the XPS and TPR analyses of the samples.

References

[1] IPCC, in: B. Metz, O. Davidson, H.C. de Coninck, M. Loos, L.A. Meyer (Eds.), Special Report on Carbon Dioxide Capture and Storage, Prepared by Working Group III of the Intergovernmental Panel on Climate Change, Cambridge University Press, Cambridge, United Kingdom/New York, NY, USA, 2005.
[2] J. Adánez, A. Abad, F. García-Labiano, P. Gayán, L.F.d. Diego, Progress in Energy and Combustion Science 38 (2012) 215–282.
[3] M.M. Hossain, H.I. de Lasa, Chemical Engineering Science 63 (2008) 4433–4451.
[4] A. Lyngfelt, M. Johansson, T. Mattisson, 9th International Conference on Circulating Fluidized Beds (CFB-9), Hamburg, Germany, 2008.
[5] J. Adánez, L.F. de Diego, F. García-Labiano, P. Gayán, A. Abad, J.M. Palacios, Energy and Fuels 18 (2004) 371–377.
[6] J. Adánez, F. García-Labiano, L.F. De Diego, P. Gayán, J. Celaya, A. Abad, Industrial and Engineering Chemistry Research 45 (2006) 2617–2625.
[7] M. Ishida, M. Yamamoto, T. Ohba, Energy Conversion and Management 43 (2002) 1469–1478.
[8] E. Jerndal, T. Mattisson, I. Thijs, F. Snijkers, A. Lyngfelt, International Journal of Greenhouse Gas Control 4 (2010) 23–35.
[9] R. Villa, C. Cristiani, G. Groppi, L. Lietti, P. Forzatti, U. Cornaro, S. Rossini, Journal of Molecular Catalysis A – Chemical 204–205 (2003) 637–646.
[10] T. Mattisson, M. Johansson, A. Lyngfelt, Fuel 85 (2006) 736–747.
[11] D. Bucker, D. Holmberg, T. Griffin, Carbon Dioxide Capture for Storage in Deep Geological Formations – Results from the CO_2 Capture Project, Elsevier, Oxford, 2005.
[12] A. Lyngfelt, B. Kronberger, J. Adánez, J.X. Morin, P. Hurst, E.S. Rubin, D.W. Keith, C.F. Gilboy, M. Wilson, T. Morris, J. Gale, K. Thambimuthu, Greenhouse Gas Control Technologies 7, Elsevier Science Ltd., Oxford, 2005, pp. 115–123.
[13] D. Hebden, H. Stroud, Chemistry of Coal Utilization, John Wiley & Sons, New York, 1981.
[14] E. Jerndal, T. Mattisson, A. Lyngfelt, Chemical Engineering Research and Design 84 (2006) 795–806.
[15] B. Wang, R. Yan, D.H. Lee, D.T. Liang, Y. Zheng, H. Zhao, C. Zheng, Energy and Fuels 22 (2008) 1012–1020.
[16] R.D. Solunke, G. Veser, Fuel 90 (2011) 608–617.
[17] R.D. Solunke, G. Veser, Energy and Fuels 23 (2009) 4787–4796.
[18] H. Tian, T. Simonyi, J. Poston, R. Siriwardane, Industrial and Engineering Chemistry Research 48 (2009) 8418–8430.
[19] L. Shen, Z. Gao, J. Wu, J. Xiao, Combustion and Flame 157 (2010) 853–863.
[20] E. Ksepko, R.V. Siriwardane, H. Tian, T. Simonyi, J.A. Poston Jr., A. Zinn, M. Sciazko, Les Rencontres Scientifiques de l'IFP – 1st International Conference on Chemical Looping, Lyon, Francia, 2010.

[21] C.R. Forero, P. Gayán, F. García-Labiano, L.F. de Diego, A. Abad, J. Adánez, International Journal of Greenhouse Gas Control 4 (2010) 762–770.
[22] K. Mayer, 3rd High Temperature Solid Looping Network Meeting, 30th August–1st September, Vienna (Austria), 2011.
[23] J. Adanez, C. Dueso, L.F. de Diego, F. Garcia-Labiano, P. Gayan, A. Abad, Energy and Fuels 23 (2009) 130–142.
[24] C. Dueso, F. García-Labiano, J. Adánez, L.F. de Diego, P. Gayán, A. Abad, Fuel 88 (2009) 2357–2364.
[25] J. Adánez, C. Dueso, L.F. de Diego, F. García-Labiano, P. Gayán, A. Abad, Industrial and Engineering Chemistry Research 48 (2009) 2509–2518.
[26] F. Garcia-Labiano, L.F. de Diego, P. Gayan, J. Adanez, A. Abad, C. Dueso, Industrial and Engineering Chemistry Research 48 (2009) 2499–2508.
[27] P. Gayán, C. Dueso, A. Abad, J. Adánez, L.F. de Diego, F. García-Labiano, Fuel 88 (2009) 1016–1023.
[28] L.F. de Diego, P. Gayán, F. García-Labiano, J. Celaya, A. Abad, J. Adánez, Energy and Fuels 19 (2005) 1850–1856.
[29] HSC Chemistry 6.1, Chemical Reaction and Equilibrium Software with Thermochemical Database and Simulation Module, Oututec Research, Pori, Finland, 2008.
[30] C. Li, Y.-W. Chen, Thermochimica Acta 256 (1995) 457–465.
[31] B. Mile, D. Stirling, M.A. Zammitt, A. Lovell, M. Webb, Journal of Catalysis 114 (1988) 12.
[32] A. Kadkhodayan, A. Brenner, Journal of Catalysis 117 (1989) 10.
[33] F. Patcas, D. Honicke, Catalysis Communications 6 (2005) 4.
[34] J. Wang, L. Dong, Y. HU, G. Zheng, Z. Hu, Y. Cheng, Journal of Solid State Chemistry 157 (2001) 274–282.
[35] C. Dueso, A. Abad, F. García-Labiano, L.F. de Diego, P. Gayán, J. Adánez, A. Lyngfelt, Fuel 89 (2010) 3399–3409.
[36] J.N. Kuhn, N. Lakshminarayanan, U.S. Ozkan, Journal of Molecular Catalysis A – Chemical 282 (2008) 12.
[37] P. Afanasiev, Applied Catalysis A – General 303 (2006) 110–115.
[38] C.D. Wagner, A.V. Naumkin, A. Kraut-Vass, J.W. Allison, C.J. Powell, J.R. Rumble, NIST, National Institute of Standards and Technology, 2003.
[39] C.D. Wagner, W.M. Riggs, L.E. Davis, J.F. Moulder, Handbook of X-ray Photoelectron Spectroscopy, Perkin-Elmer Corp., 1979.
[40] A.N. Buckley, R. Woods, Journal of Molecular Catalysis A – Chemical 21 (1991) 575–582.
[41] P.J. Mangnus, E.K. Poels, A.D.V. Langeveld, J.A. Moulijn, Journal of Catalysis 137 (1992) 92–101.
[42] S.P.A. Louwers, R. Prins, Journal of Catalysis 133 (1992) 94–111.
[43] P. Arnoldy, J.A.M.V.D. Heijkant, D.D.d. Bok, J.A. Moulijn, Journal of Catalysis 92 (1985) 35–55.